

# First Stage Experiment on Optical Diffraction Radiation at KEK-ATF: Theoretical Approach.

P. Karataev<sup>a</sup>, S. Araki<sup>b</sup>, R. Hamatsu<sup>a</sup>, H. Hayano<sup>b</sup>, T. Hirose<sup>a</sup>, T. Muto<sup>a</sup>, T. Naito<sup>b</sup>,  
G. Naumenko<sup>c</sup>, A. Potylitsyn<sup>c</sup>, J. Urakawa<sup>b</sup>

<sup>a</sup> *Tokyo Metropolitan University, 1-1 Minamiohsawa, Hachioji, Tokyo 192-0937, Japan*

<sup>b</sup> *KEK: High Energy Accelerator Research Organization  
, Oho 1-1, Tsukuba, 305-0801, Ibaraki - ken, Japan*

<sup>c</sup> *Tomsk Polytechnic University, 634050, pr. Lenina 2a, Tomsk, Russia*

---

Extremely low emittance and high current electron beam is one of the vital characteristics for linear colliders or X-ray FEL's. Parallel developments of non-invasive beam diagnostics are strongly required for realizing such beams. Detection of Optical Diffraction Radiation (ODR), because of its non-destructive nature, is the most promising technique for the application to the non-invasive beam diagnostics; however, very little experimental investigations existed.

Up to now Transition Radiation (TR) has widely been used for non-invasive beam diagnostics. That is because of high signal-to-noise ratio, instantaneous emission, large emission angles, and availability of detailed comparison with the theory. But in this case the particle directly interacts with a target that may lead to emittance growth.

At KEK-ATF Damping Ring detailed investigation of Optical Diffraction Radiation is planned. The optimization of experimental conditions is required.

A model for calculating the ODR characteristics from an ultrarelativistic charged particle distributed by Gaussian law and moving close to a tilted conducting screen has been developed. It is noticed that at the impact parameter (shortest distance between the particle trajectory and the target) comparable with beam size the TR is significant. Results of simulations based on the experimental conditions are also shown.

---

# 1. Introduction

Recent years have witnessed an intense study of both linear colliders (LC) with energy of a few hundred GeV and X-ray free-electron lasers (FEL). The extremely low emittance and high brightness beam is one of the vital characteristics of them. For example, generation of high intense gamma beams based on Compton backscattering requires lower emittance to achieve higher luminosity [1], and in FEL the low emittance is required to decrease the radiation distribution delusion and enhance the intensity [2]. Therefore, a full characterization of beam size, angular divergence, length, etc. is required to optimize accelerator performance. But a simple non-invasive method is still absent.

During last several years both incoherent and coherent transition radiation (TR) appearing when a charged particle crosses a boundary between two media with different dielectric properties has widely been used for transversal and longitudinal beam size characterization in linac type accelerators [3-6]. That is because of well-known TR features: high signal-to-noise ratio which reduces requirements to detection apparatus, instantaneous emission allowing time-resolved measurements, possibility of detailed comparison of experiment and theory that increases the accuracy of the method, large observation angles allowing radiation registration at good background conditions. However, generating TR the particles directly interact with the target. It may lead to significant emittance growth in case of a thick target. That is the problem of all destructive methods like wire scanners or second emission monitor grids. In case of a thin TR radiator [6] the interaction of a high current electron beam with the target material may lead to deformation or destruction of the target due to the ionization heating process and, therefore, embarrass the result interpretation.

Diffraction radiation (DR) appearing when a charged particle beam moves in the vicinity of a conducting target is one of the promising techniques for non-invasive beam diagnostics as the particles do not directly interact with a target. The first theoretical considerations of DR have appeared about 40 years ago [7-8]. Recent papers considered DR properties [9-11] and their implementation to beam diagnostics [12-14] in details. But there are only four experimental papers [15-18] (in our knowledge). The first observation of coherent DR (CDR) (when wavelength is comparable or longer than the longitudinal beam size) in millimeter and sub-millimeter wavelength region has been performed in 1995 [15]. The authors have presented the investigation of forward CDR (emitted along the particle trajectory) superposed with coherent TR (CTR) from a pickoff mirror installed downstream the target. The pickoff mirror also intercepted the electron beam parameters. The use of backward DR (emitted along the mirror reflection direction from the target) is more preferable because of large emission angles. In [16-17] the authors presented the backward CDR investigation and evaluation of longitudinal beam size using autocorrelation technique. They noted that in their case the existing theory must be improved due to the approximations involved: infinite target size and far-field approximation.

One important aspect common to the papers [15-17] is that they investigated coherent DR in order to be able to determine longitudinal beam shape. The beam length is usually much larger than transversal size. As is shown below, DR is more sensitive to transversal beam sizes at shorter wavelengths. The modern detection apparatus allows registering optical radiation with marvelous accuracy. Thus, we assume that Optical Diffraction Radiation (ODR) as a basis for beam diagnostics may be a very precise tool for future linear

colliders and FELs.

Table 1: Characteristics of KEK-ATF damping ring.

<b>Maximum energy</b>		1.28 GeV ( $\gamma = 2500$ )
<b>Beam emittance</b>	Vertical	$(1.5 \pm 0.25) \times 10^{-11}$ m rad
	Horizontal	$(1.4 \pm 0.3) \times 10^{-9}$ m rad
<b>Vertical beam size (near the ODR target)</b>		$\sigma_y \sim 10\mu$
<b>Horizontal beam size (near the ODR target)</b>		$\sigma_x \sim 100\mu$
<b>Bunch length</b>		$\sim 6$ mm
<b>Single-bunch population</b>		$1.2 \times 10^{10}$

There is only one experimental paper on ordinary ODR observation at internal beam of Tomsk synchrotron “Sirius” [18]. At KEK-ATF Damping Ring Extracted Beam, whose characteristics are presented in Table 1, we are going to investigate Optical Diffraction Radiation (ODR) as a possible tool for non-invasive beam diagnostics in details in frame of collaboration [19]. We assume that it is rather risky to develop a complete device for ODR based beam diagnostics without investigating the basic characteristics of it.

The first stage experiment supposes investigation of optical system and ODR characteristics from a target with large transversal size (semi-plane target). The purpose of the report is to review the existed theory and to perform calculations for a real experimental situation taking into account the experimental experience of the scientific groups dealt with transition and diffraction radiation effects.

## 2. Theoretical Review

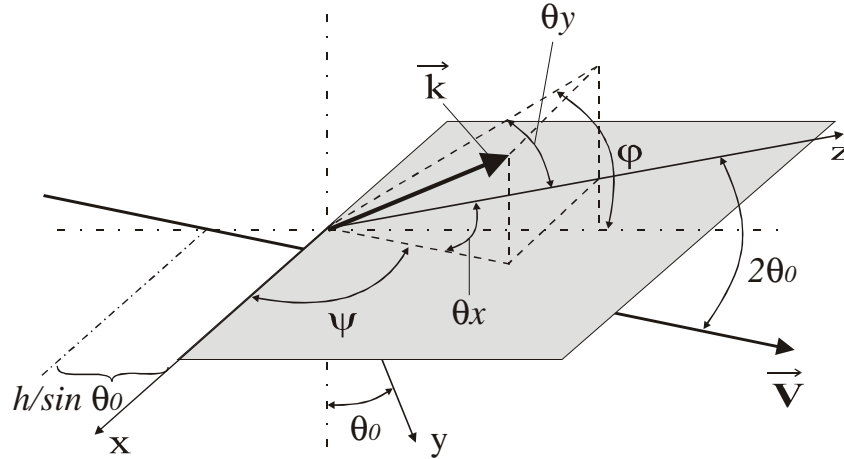


Fig. 1: Diffraction Radiation production. Z-axis is directed along the mirror reflection direction and X-axis – along the target edge.

Diffraction radiation appears when a charged particle moves rectilinearly and with

constant velocity in the vicinity of a medium (target) with impact parameter (the shortest distance between the particle trajectory and the target edge)  $h$  (see Fig.1):

$$h \leq \frac{\gamma\lambda}{2\pi} \quad (1).$$

Here  $\gamma = E/m_e c^2 = (1 - \beta^2)^{-1/2}$  is the charged particle Lorentz-factor,  $\beta$  is the particle velocity in units of light velocity in vacuum,  $\lambda$  is the observation wavelength.

The passing particle interacts with the target with its electric field inducing currents changing in time. These currents give rise in the radiation. In obvious analogy with TR if the particle moves close to a plane target, DR has a tendency to propagate in two main directions: along the particle trajectory (Forward Diffraction Radiation, FDR) and in the direction of mirror reflection (Backward Diffraction Radiation, BDR).

An exact solution of Maxwell's equations for DR spectral angular density has been derived in [8]:

$$\begin{aligned} \frac{d^2 W_{DR}(h)}{d\omega d\Omega} &= \frac{\alpha}{2\pi^2} \frac{\exp\left(-\omega/\omega_c \sqrt{1 + \beta^2 \gamma^2 \cos^2 \psi}\right)}{\sin \psi} \\ &\times \left\{ \cos^2 \frac{\varphi}{2} \cos^2 \psi (1 - \beta \sin \psi \cos \theta_0) + (\gamma^{-2} + \beta^2 \cos^2 \psi) \sin^2 \frac{\varphi}{2} (1 + \beta \sin \psi \cos \theta_0) \right\} \quad (2). \\ &\times \left\{ (\gamma^{-2} + \beta^2 \cos^2 \psi) \left[ \left( \sin \psi \cos \varphi - \frac{\cos \theta_0}{\beta} \right)^2 + \frac{(\gamma^{-2} + \beta^2 \cos^2 \psi) \sin^2 \theta_0}{\beta^2} \right] \right\}^{-1} \end{aligned}$$

Here  $\alpha$  is the fine structure constant;  $\omega = 2\pi/\lambda$  is the radiation energy (throughout the paper  $h = m_e = c = 1$ );  $\omega_c = \gamma/2|h|$  is the DR characteristic energy;  $\psi$  and  $\varphi$  are the azimuthal and polar outgoing angles with respect to the target plane (see Fig. 1),  $\theta_0$  is the target tilt angle with respect to the particle trajectory.

To be able to obtain the exact solution [8], the authors involved the following approximations:

1. Impact parameter must be larger than the observation wavelength ( $h > \lambda$ ) (classical electrodynamics approximation [9]);
2. Infinitely thin and ideally flat target;
3. Perfectly conducting target material;
4. Far-field approximation.

But the model is applicable for any electron energies and any observation angles.

Many scientists [10-14] suppose that the use of observation angles with respect to the mirror reflection direction from the target makes the understanding of the effect simpler. To transform the Eq. (2) to mirror reflection observation geometry, it is necessary to make the following substitution [10]:

$$\psi = \frac{\pi}{2} - \theta_x; \quad \varphi = \theta_y + \theta_0 \quad (3),$$

where  $\theta_x$  and  $\theta_y$  are the radiation angles measured from mirror reflection direction (see Fig.1).

The angular distribution of diffraction radiation is presented in Fig. 2 (solid line). Zero angle corresponds to mirror reflection direction. It is obvious that the DR as well as TR [9] is concentrated in a cone of order of  $\gamma^{-1}$ . An ultrarelativistic approximation [10] ( $\gamma \gg 1$ ) allows considering angular range

$$\theta_y, \theta_x \sim \gamma^{-1} \ll 1; \quad (4).$$

Substituting (3) into (2) and using ultrarelativistic approximation (4) we have (neglecting the terms higher than  $\gamma^{-2}$ ):

$$\frac{d^2 W_{DR}(h)}{d\omega d\Omega} = \frac{\alpha}{4\pi^2} \exp\left(-\frac{\omega}{\omega_c} \sqrt{1 + \gamma^2 \theta_x^2}\right) \frac{\gamma^{-2} + 2\theta_x^2}{(\gamma^{-2} + \theta_x^2)(\gamma^{-2} + \theta_x^2 + \theta_y^2)} \quad (5).$$

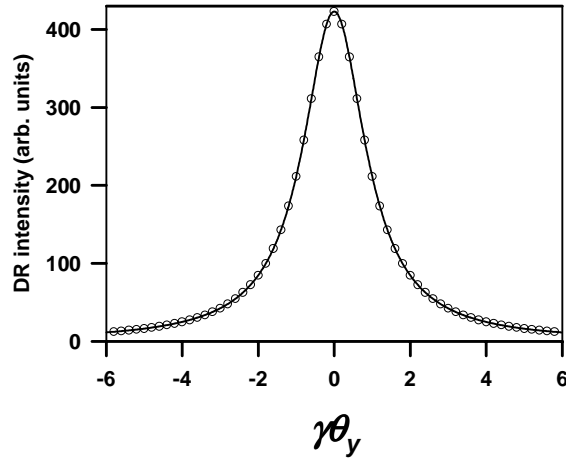


Fig.2: Diffraction radiation angular distributions calculated using Eqs. (2) (solid line) and (5) (circles). Parameters:  $\gamma = 2500$ , (1.28 GeV – KEK-ATF Damping Ring energy),  $h = 0.1\text{mm}$ ,  $\theta_x = 0$ ,  $\lambda = 500\text{nm}$ .

The DR angular distribution calculated using Eq. (5) is also presented in Fig. 2. The agreement of the distributions for chosen parameters (see figure caption) shows the validity of ultrarelativistic approximation.

One can see that in contrast to TR the DR distribution have the only maximum at  $\theta_x = \theta_y = 0$ :

$$\frac{d^2 W_{\max}(h)}{d\omega d\Omega} = \frac{\gamma^2 \alpha}{4\pi^2} \exp\left(-\frac{\omega}{\omega_c}\right) \quad (6)$$

whose magnitude differs from the maximal value of the TR intensity by an exponential term [10].

Integrating (5) [10] over energy and observation angles one can derive the radiation loss  $W$  of the passing particle due to BDR process:

$$W = \frac{3}{8} \alpha \omega_c = \frac{3}{8} \alpha \frac{\gamma}{2h} \quad (7).$$

The total radiation loss is equal to doubled value (6) due to sum of BDR and FDR contribution. The model described above is the classical theory of diffraction radiation. The purpose of the paper is to prepare the model for later comparison with experimental results. There are two possible ways to achieve a good coincidence of experiment and theory. The first one is to approve theoretical approach making it closer to a real experimental situation (for example, to take into account angular resolution, optical filter bandwidth, etc.). The second way is to approve experimental conditions (for example, target quality or optical system accuracy). We must consider both ways to later achieve a good accuracy of DR based diagnostics [19].

An electron beam has transversal size. When it moves in the vicinity of the target, a part of it produces TR (see Fig. 3a). Therefore, the first step to making the theory closer to a real situation is to take into account the contribution of TR produced by the beam tails.

TR and DR are two particular cases of *polarization radiation* as they are produced as a result of dynamical polarization of a medium. Sometimes, describing a situation when TR and DR appear together, we shall call the effect as *polarization radiation* (PR).

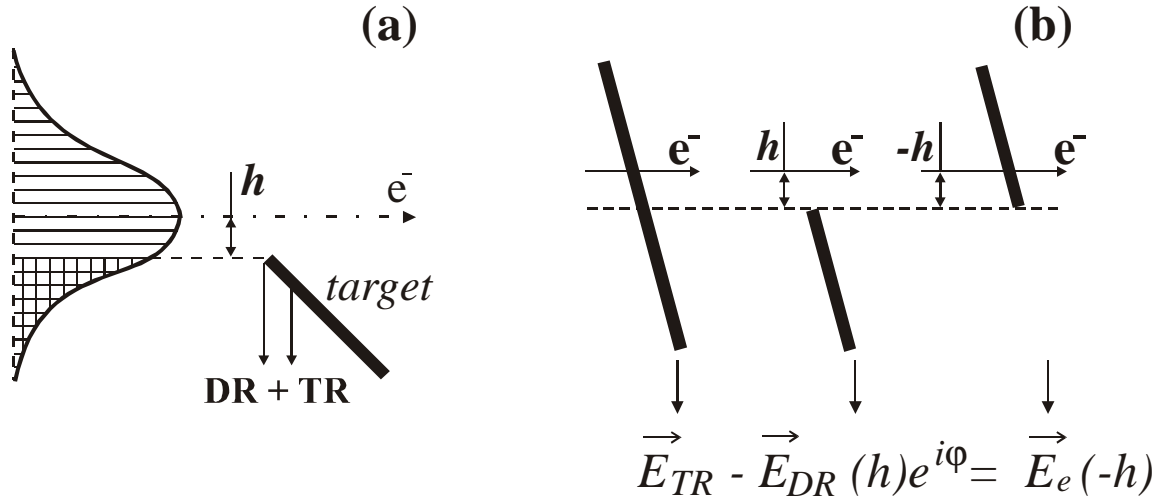


Fig. 3: Geometry of a beam tail TR contribution (a) and relation between fields of infinite target TR  $\vec{E}_{TR}$ , DR from a semi-plane  $\vec{E}_{DR}$  (edge transition radiation, ETR), and finite target TR  $\vec{E}_e$  (b).

According to [10] the TR electric field strength for a particle moving through a semi-plane can be derived using well-known Babinet's principle from classical optics:

$$\vec{E}_e(-h) = \vec{E}_{TR} - \vec{E}_{DR}(h)e^{i\varphi} \quad (8),$$

where  $\vec{E}_{TR}$  is the TR electric field strength for an infinite boundary,  $\vec{E}_{DR}$  is the DR field from a semi-plane, and  $\vec{E}_e$  is the edge TR (ETR) field from a particle moving trough the finite size target (the negative sing of  $h$  shows that the particle moves through the target). One may see that in contrast to [10], where one of the present paper authors considered a traditional spot TR approach, the Eq. (8) contains the exponential terms with the phase shift

$\varphi = \frac{\omega}{2\omega_c} \gamma \theta_y$  determined by the time difference between the waves being formed in the vicinity of the target edge and at the point where the target crosses the target plane [20]. If the interaction point is close to the target edge, the phase shift plays significant role and cannot be neglected. Therefore, the traditional theory of a spotlike TR must be revised for the considered case.

The TR electric field strength from an infinite boundary in ultrarelativistic case has a well-known form [9]:

$$\vec{E}_{TR\ x,y} = \frac{ie}{2\pi^2} \frac{\theta_{x,y}}{\left(\gamma^{-2} + \theta_x^2 + \theta_y^2\right)} \quad (9).$$

In (9)  $e$  is the electron charge,  $x$  or  $y$  is the horizontal or vertical polarization components respectively.

The two polarization components of DR may be represented in the following form:

$$\begin{aligned} \vec{E}_{DR\ x}(h) &= \frac{ie}{4\pi^2} \frac{\theta_x}{\sqrt{\gamma^{-2} + \theta_x^2}} \frac{\exp\left[-\frac{\omega}{2\omega_c} \sqrt{1 + \gamma^2 \theta_x^2}\right]}{\sqrt{\gamma^{-2} + \theta_x^2} - i\theta_y} \\ \vec{E}_{DR\ y}(h) &= \frac{ie}{4\pi^2} \frac{\exp\left[-\frac{\omega}{2\omega_c} \sqrt{1 + \gamma^2 \theta_x^2}\right]}{-i\sqrt{\gamma^{-2} + \theta_x^2} + \theta_y} \end{aligned} \quad (10).$$

Substituting the Eqs. (9) and (10) in (8) one may obtain spectral angular distribution for TR including edge conditions:

$$\begin{aligned} \frac{d^2W_e(-h)}{d\omega d\Omega} &= 4\pi^2 \left( \left| \vec{E}_{e,x} \right|^2 + \left| \vec{E}_{e,y} \right|^2 \right) = \frac{\alpha}{\pi^2} \frac{\theta_x^2 + \theta_y^2}{\left(\gamma^{-2} + \theta_x^2 + \theta_y^2\right)^2} \\ &\times \left\{ 1 + e^{-2a} \frac{\left(\gamma^{-2} + \theta_x^2 + \theta_y^2\right)\left(\gamma^{-2} + 2\theta_x^2\right)}{4\left(\theta_x^2 + \theta_y^2\right)\left(\gamma^{-2} + \theta_x^2\right)} - e^{-a} \left[ \cos\varphi + \frac{\theta_y}{\left(\theta_x^2 + \theta_y^2\right)} \frac{\left(\gamma^{-2} + 2\theta_x^2\right)}{\sqrt{\gamma^{-2} + \theta_x^2}} \sin\varphi \right] \right\} \end{aligned} \quad (11).$$

In (11)  $a = \frac{\omega}{2\omega_c} \sqrt{1 + \gamma^2 \theta_x^2}$ .

One may see that Eq. (11) differs from classical TR by a term in the brackets. If the impact parameter being contained in the decay factor  $a$  tends to infinity, the term in brackets tends to unity, and, therefore, the Eq. (11) is transformed to the classical TR spectral angular distribution which is well described in [9].

Finally, the expression for polarization radiation may be written in the following form:

$$\frac{d^2W_{PR}(h)}{d\omega d\Omega} = \begin{cases} \frac{d^2W_{DR}(h)}{d\omega d\Omega}, & h \geq 0 \\ \frac{d^2W_e(-h)}{d\omega d\Omega}, & h \leq 0 \end{cases} \quad (12).$$

Here negative impact parameter corresponds to the semi-plane TR, and positive impact parameters – to DR. In the case of  $h = 0$  the Eqs. (5) and (11) coincide. Such representation allows us to join two models for DR and ETR and call as polarization radiation (PR).

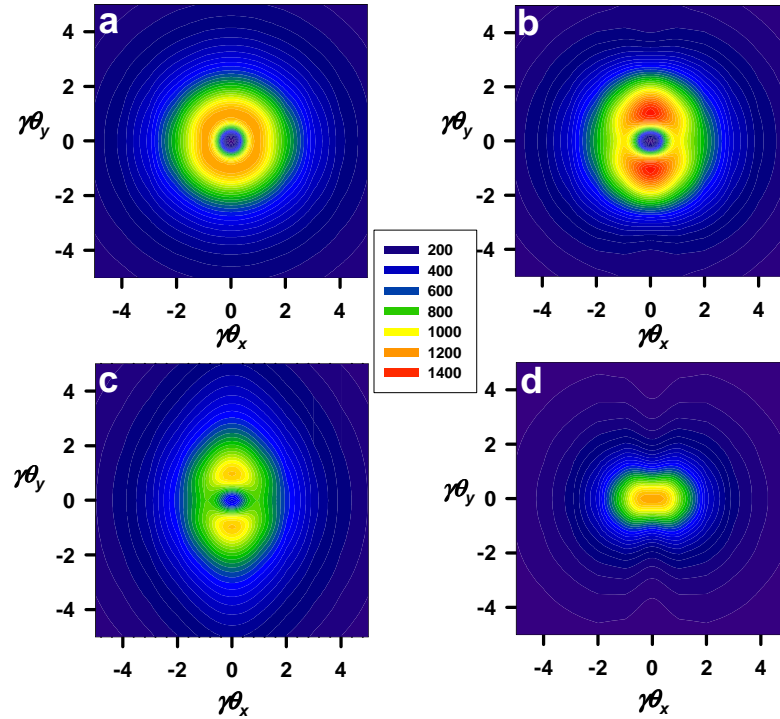


Fig. 4: Effect of azimuthal asymmetry in case of edge transition radiation: a)  $-h \rightarrow \infty$ ; b)  $-h = 3\gamma\lambda / 4\pi$ ; c)  $-h = \gamma\lambda / 4\pi$ ; d)  $h = 0$  (parameters of the Fig. 2).

Fig. 4 shows the angular distribution of TR in the vicinity of the target edge. One can see that in contrast to classical TR (Fig. 4a) an azimuthal asymmetry appears in ETR angular distribution at  $h \leq \gamma\lambda$ . In case of impact parameter  $h \approx \frac{3\gamma\lambda}{4\pi}$  the edge TR intensity in the diffraction plane ( $\theta_x = 0$ ) exceeds the level of classical TR on about 25%, on the other hand, in the plane perpendicular to the diffraction one ( $\theta_y = 0$ ) the TR intensity is significantly suppressed. The effect of azimuthal asymmetry may be very useful for beam size diagnostics as it strongly depends on the impact parameter. Fig. 5 shows an example of the polarization radiation dependence on the impact parameter.  $h = 0$  corresponds to the target edge.

Negative impact parameters correspond to the edge TR and positive – to DR.

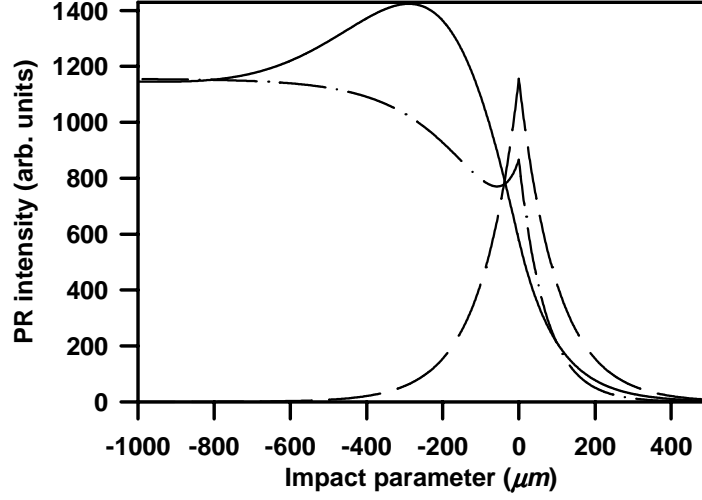


Fig. 5: Distribution of polarization radiation: solid line -  $\theta_x=0$ ,  $\theta_y=1/\gamma$ ; dashed line -  $\theta_x=0$ ,  $\theta_y=0$ ; dashed-dotted line -  $\theta_x=0$ ,  $\theta_y=1/\gamma$ (parameters of the Fig.2).

Assuming that the electrons in a beam are distributed by Gauss' law:

$$G(\bar{h} - \delta h) = \frac{1}{\sigma_y \sqrt{2\pi}} \exp\left(-\frac{(\bar{h} - \delta h)^2}{2\sigma_y^2}\right) \quad (13)$$

where  $\sigma_y$  is the transversal beam size and  $\bar{h}$  is the position of the beam center with respect to the target edge (see Fig. 3), one may write an entire expression for polarization radiation accounting TR from beam tails in the form:

$$\begin{aligned} \overline{\frac{d^2 W_{PR}(\bar{h}, \sigma_y)}{d\omega d\Omega}} &= \int_0^{\infty} \frac{d^2 W_{DR}(\delta h)}{d\omega d\Omega} G(\bar{h} - \delta h) d\delta h + \int_{-\infty}^0 \frac{d^2 W_e(-\delta h)}{d\omega d\Omega} G(\bar{h} - \delta h) d\delta h = \\ &= \int_0^{\infty} \left\{ \frac{d^2 W_{DR}(\delta h)}{d\omega d\Omega} G(\bar{h} - \delta h) + \frac{d^2 W_e(\delta h)}{d\omega d\Omega} G(\bar{h} + \delta h) \right\} d\delta h \end{aligned} \quad (14).$$

Integrating two terms in Eq. (14) separately over all angular and optical energy range one may obtain the total number of optical photons of TR and DR produced by a bunch of electrons distributed by the Gauss law. The integrating results are presented in Fig. 6. It is apparent that the total number of TR photons smoothly decreases when increasing the impact parameter. At the distance from the target of  $2.5\sigma_y$  ( $25\mu$  for our case) the contribution of TR is less than 1% and may be neglected. One should notice that the beam tail shape may not obey the Gauss law. Therefore, the impact parameter for estimations is chosen at  $h = 100\mu$  in

order to reduce possible contribution of OTR from non-gaussian beam tails. In this case the number of ODR photons is of order of  $10^7$  per bunch containing  $10^{10}$  electrons.

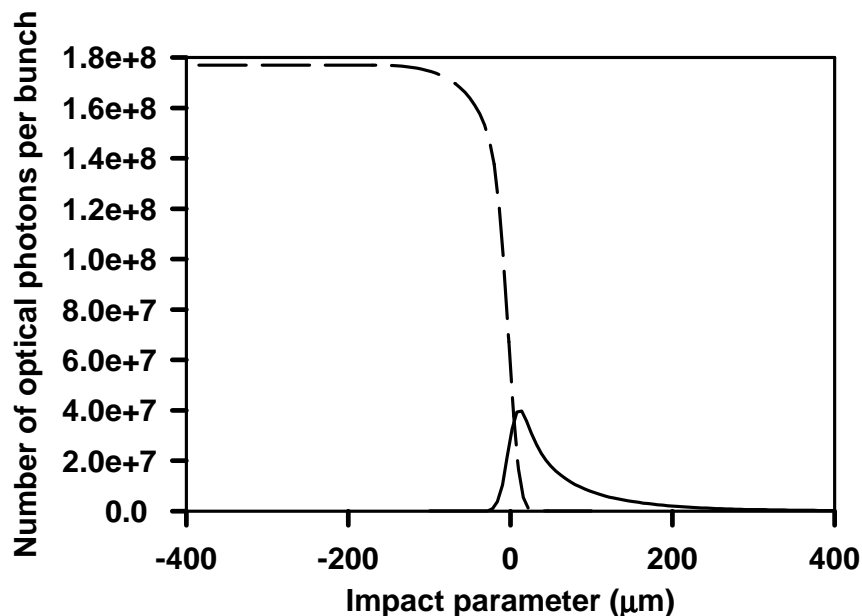


Fig. 6: Distribution of the total number of optical photons as a function of impact parameter corresponding to DR (solid line) and TR processes per bunch containing  $10^{10}$  electrons calculated for the beam size  $\sigma_y = 10\mu$ .

The Eq. (14) has been used for further calculations. To make the estimations for our experimental set-up, it is necessary to describe the characteristics of it first.

### 3. Experimental conditions and estimations.

The experimental set-up for ODR investigations is described in details in [22]. In this section we are going to explain the parameters of the optical system and perform estimations according to them.

In contrast to [15-17] the ODR angular characteristics bear information about transversal beam parameters. Fig. 7a shows angular distribution of ODR for different beam sizes calculated with Eq. (14). When increasing the beam size the ODR peak intensity increases. It happens because more particles of the beam move closer to the target. Actually, more particles move with longer distance to the target, but the contribution of the close particles surpasses the distant ones [11]. Thus, the angular characteristics must be precisely measured to achieve a better accuracy of diagnostic method [19].

The choice of angular acceptance:

$$\Delta\theta_y = \Delta\theta_x = 0.2 \frac{1}{\gamma} = 0.08 \text{ mrad} \quad (15)$$

does not lead to significant distortion of ODR angular distribution.

Fig. 7b depicts the dependences of the ODR peak intensity on the beam size normalized

by their minimal value. This dependence is shown as an example. Of course, DR angular distribution from a slit target strongly depends on beam parameters. One can see that the ODR is better sensitive to beam size at shorter wavelength and, therefore, the optical filter bandwidth also plays significant role. From Eq. (5) it is obvious that the DR intensity exponentially decreases with increasing the radiation energy. We assume that modern apparatus registers optical radiation with a very good accuracy and ODR based diagnostics can be a very precise technique.

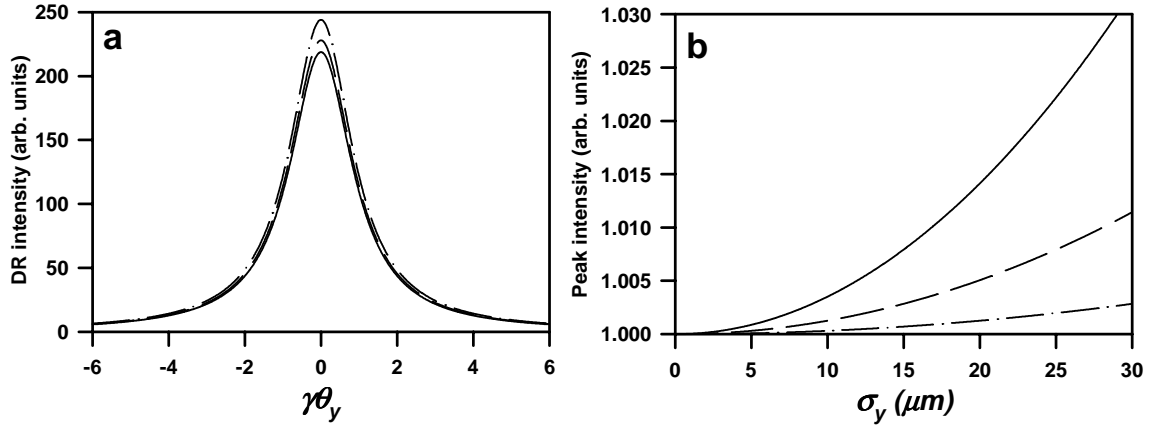


Fig. 7: a) DR angular distribution: solid line -  $\sigma_y = 10\mu\text{m}$ , dashed line -  $\sigma_y = 20\mu\text{m}$ , dashed-dotted line -  $\sigma_y = 30\mu\text{m}$ ; b) DR peak intensity as a function of the beam size: solid line -  $\lambda = 300\text{nm}$ , dashed line -  $\lambda = 500\text{nm}$ , dashed-dotted line -  $\lambda = 1000\text{nm}$ .

For our estimations we chose optical filters with 10% bandwidth. Choosing a high angular and energy resolution leads to reducing the number of photons. In this case the sensitivity of the detection apparatus influences on the registration efficiency.

Fig. 8 shows the angular distribution of the number of ODR photons in the diffraction plane taking into account the narrow acceptance (15) and 10% bandwidth of 500nm optical filter. One can see that the maximal number of photons is of order of  $10^4$  photons per bunch containing  $10^{10}$  electrons. Such intensity can be easily detected by a photomultiplier or intensified CCD camera.

The model described above contains approximations. The authors of [17] noticed the inapplicability of existing theory due to such approximations as far field and infinite target size.

In obvious analogy with edge transition radiation the diffraction radiation spectral angular distribution may also be distorted if the target size is comparable or less than  $\gamma\lambda$  - effective electron field width as a result of appearing another edge condition. Therefore, to obey the infinite target size approximation, the following condition must be fulfilled:

$$a \gg \gamma\lambda \quad (16),$$

where  $a$  is the target width.

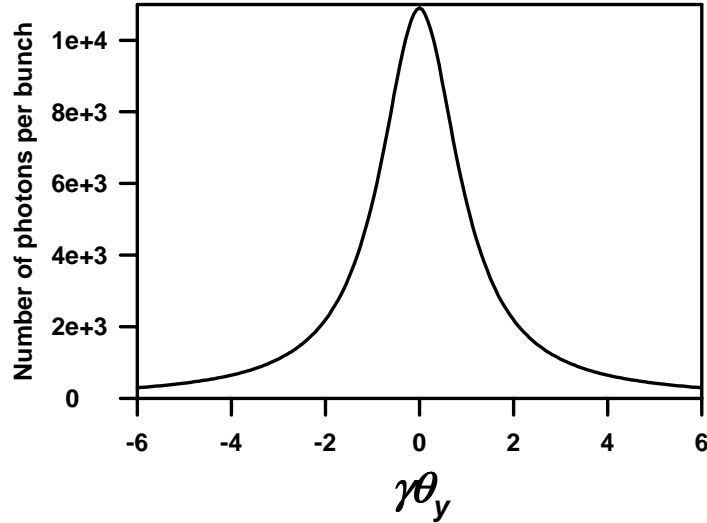


Fig. 8: Angular distribution of the number of ODR photons in the diffraction plane ( $\theta_x = 0$ ) from an electron beam with  $\sigma_y = 10\mu\text{m}$  and population of  $10^{10}$  e/bunch calculated using Eq. (14) accounting narrow angular acceptance  $\Delta\theta_x = \Delta\theta_y = 0.2/\gamma = 80\mu\text{rad}$  and 10% bandwidth for  $\lambda = 500\text{nm}$ .

In [17] the coherent diffraction radiation in millimeter and submillimeter wavelength region has been investigated. In their case  $\gamma\lambda$  is in the range of  $900 \div 1350\text{mm}$ . Of course, it is a rather complicated task to obey condition (16), consequently, the theoretical approach must be improved (see for instance [23]). In our case the parameter  $\gamma\lambda$  varies from 0.75 to 2mm. Thus, even 10mm target size obeys the infinite target size approximation. From this point of view the target of  $100\mu\text{m}$  thick has been chosen. Both in [8] and [9] the models have been derived for infinitely thin target. That means that only the surface current component induced by the passing particle gives rise in the radiation. But in reality a target has a finite thickness. The current component perpendicular to the target surface may also give rise in the radiation, which may destructively interfere with the surface one. We assume that the contribution of the perpendicular current component is negligibly small if the target thickness is much smaller than  $\gamma\lambda$ .

The model described above has been derived in the frame of far field approximation. That means that the radiation source size is treated like a point. But in reality, the DR as well as TR [24] source sizes are not zero. To obey the far field approximation, the following condition must be fulfilled:

$$L \gg \gamma^2 \Delta \quad (17).$$

In (17)  $L$  is the target detector distance and  $\Delta = \lambda/2\pi$  is the reduced wavelength. The parameter  $\gamma^2 \Delta$  is treated as the radiation formation length [24], the distance from the target where the radiation source size may be considered as a point. In [24] the authors considered the importance of the TR source size contribution for OTR based beam size diagnostics. They noticed that the TR angular distribution containing the central minimum and the ring

with the  $l/\gamma$  radius (see Fig. 4a) may be replaced by a wider structure if the far field condition is not fulfilled. In case of [17] the radiation formation length  $\gamma^2 \Delta$  is in the range of 64 ÷ 100m. Such distance may even exceed the laboratory size. Again the theoretical approach must be improved. In our case the parameter  $\gamma^2 \Delta$  varies from 0.3 to 0.8m. For the experimental setup presented in [22] we chose the target detector distance  $L = 2\text{m}$  and had foreseen a possibility for increasing.

## Conclusion

In the paper we present a model, which will be used for later comparison with the experiment. The estimations have shown that it is possible to measure ODR angular characteristics with proper accuracy. We performed detailed consideration on involved approximations and found the possibility to obey them. In [17] the authors presented the approved theoretical model, which is much more complicated. The classical DR approach is much simpler and flexible to any other mathematical transformations such as convolution with beam size distribution.

Table 2: Optical system parameters.

PARAMETER		CONDITION	VALUE
Impact parameter, $h$			$100\mu$
Angular resolution	$\Delta\theta_x$	$\leq 0.2 \gamma^{-1}$	$80\mu\text{rad}$
	$\Delta\theta_y$	$\leq 0.2 \gamma^{-1}$	$80\mu\text{rad}$
Optical filter bandwidth, $\Delta\lambda$		$\leq 10\%$	$40\div 80 \text{ nm}$
Distance: target – detector, $L$		$\gg \gamma^2 \lambda$	$2\text{m}$
Target width		$\gg \gamma \lambda$	$10\text{mm}$
Target thickness		$\ll \gamma \lambda$	$100\mu$

The chosen parameters for experimental setup are listed up in the Table 2. First of all we are going to investigate the optical system using ordinary transition radiation as it is experimentally and theoretically studied very well. If we are able to precisely measure the angular characteristics of OTR, we may expect good results for ODR measurements.

Investigation of our optical system assumes the determination of wavelength efficiency. As is well known, a photomultiplier or CCD camera may have different response for different radiation wavelengths. Also, we are going to use optical filters, which may have different transmittance or reflecting capability in case transmitting or reflecting filters respectively. For this purpose we need a source with well known spectral characteristics.

TR from a single electron is independent on energy if the far-field approximation is fulfilled [23] as the radiation source size depends on observation energy. The total TR spectrum can be presented in the following form [17]:

$$F(\omega) = I(\omega)[N + N(N - 1)S(\omega)] \quad (17),$$

where  $I(\omega)$  is the radiation intensity from a single electron,  $N$  is the number of electrons per bunch,  $\omega = 2\pi/\lambda$  is the radiation energy, and  $S(\omega)$  is the longitudinal bunch form factor, which is determined by the Fourier transform of the longitudinal electron distribution in the bunch  $G(t)$ :

$$S(\omega) = \left| \int G(t) e^{i\omega t} dt \right|^2 = e^{-4\pi^2 \frac{\sigma_z^2}{\lambda^2}} \quad (18).$$

In (17) the first term in the brackets is responsible for incoherent radiation part, and the second one is responsible for coherent radiation.

The right part of the Eq. (18) has been derived assuming that the longitudinal electron distribution obeys the Gauss' law (13). That is easy to see that if the longitudinal beam size is much larger than the observation wavelength, the bunch form factor tends to zero and contribution of the coherent radiation is negligibly small and can be neglected. Therefore, the total radiation intensity is determined by the incoherent radiation. In [16] the authors derived a simple condition for coherent radiation:

$$\sigma_z \leq \frac{\lambda}{2\pi} \quad (19).$$

The authors of [11] considered an asymmetric longitudinal beam profile. They noted that for asymmetric beam the coherent radiation contribution can be significant even at wavelength much smaller than the beam size. For weakly asymmetric beam they derived another condition

$$\sigma_z \leq \frac{\lambda}{2\pi} N^{1/6} \quad (20),$$

which is weaker than (19). But even in this case the contribution of coherent component for optical radiation and KEK-ATF parameters is negligibly small as the longitudinal beam size exceeds the condition (20) three orders. Classical OTR is the best source for wavelength efficiency measurements as its spectrum is constant.

After investigation of optical system using OTR we are going to investigate ODR and ETR from a semi-plane in details. We will estimate the applicability of the existing theory to ODR description.

The experimental conditions for a slit target will be later considered in details. The slit ODR measurement is the final goal of our investigations [19]. We assume that it is rather risky to develop a complete device for ODR based diagnostics without testing main characteristics of it.

## References

- [1] Valery Telnov, *Nucl. Instr. and Meth. A* **455** (2000) 63 and references therein.

- [2] Kwang-Je Kim, *AIP Conf. Proc.* **398** (1997) 243.
- [3] J.-I.Choi, H.S.Kang, S.H.Nam, S.S.Chang, *Proc. of the 1999 Part. Accel. Conf.*, New York, 1999, p. 2205.
- [4] P.Piot, G.A.Kraft, K.Jordan, A.Grippio, J.Song, *Proc. of the 1999 Part. Accel. Conf.*, New York, 1999, p. 2229.
- [5] J.B.Rosenzweig, A.Murokh, and A.Tremaine, *AIP Conf. Proc.* **472** (1999) 38.
- [6] P.Piot, J.-C.Denard, P.Adderley, K.Capek, E.Feldl, *AIP Conf. Proc.* **390** (1997) 298.
- [7] Yu.Dnestrovskii, D.P.Kostomarov, *Sov. Phys. Dokl.* **2** (1957) 442, *Sov. Phys. Dokl.* **4** (1959) 158.
- [8] A.P.Kazantsev, G.I.Surdutovich, *Sov. Phys. Dokl.* **7** (1963) 990.
- [9] M.L.Ter-Mikaelyan, *High Energy Electromagnetic Processes in Condensed Media* (Wiley-Interscience, New-York, 1972).
- [10] A.P.Potylitsyn, *Nucl. Instr. And Meth. B* **145** (1998) 169.
- [11] A.R.Mkrtchyan, L.A.Gevorgian, L.Sh.Grigorian, B.V.Khachatryan, A.A.Saharian, *Nucl. Instr. And Meth. B* **145** (1998) 67.
- [12] D.W.Rule, R.B. Fiorito, W.D.Kimura, *AIP Conf. Proc.* **390** (1997) 510.
- [13] M.Castellano, *Nucl. Instr. And Meth. A* **394** (1997) 275.
- [14] D.W.Rule, R.B. Fiorito, W.D.Kimura, *AIP Conf. Proc.* **472** (1999) 725.
- [15] Y.Shibata, S.Hasebe, K.Ishi, et al., *Phys. Rev. E* **52** (1995) 6787.
- [16] A.H.Lumpkin, N.S.Sereno, G.A.Decker, D.W.Rule, *AIP Conf. Proc.* **546** (2000) 484.
- [17] M.Castellano, V.A.Verzilov, L.Catani, et al., *Phys. Rev. E* **63** (2001) 056501.
- [18] I.E.Vnukov, B.N.Kalinin, G.A.Naumenko, et al., *JETP Lett.* **67** (1998) 802.
- [19] J.Urakawa, H.Hayano, et al., "Investigation of Optical Diffraction Radiation as a Basis for a New Non-Invasive Beam Diagnostics", KEK-report, Internal 2000-5, August, 2000.
- [20] A.Potylitsyn, P.Karataev, G.Naumenko, *Phys. Rev. E* **61** (2000) 7039.
- [21] H.Hayano, K.kubo, M.Ross, et al., "ATF: Accelerator Test Facility Study Report JFY 1996-1999", KEK-report, Internal 2000-6, August 2000, A.
- [22] T.Muto, S. Araki, R. Hamatsu, et al., "First stage experiment at KEK-ATF", ICFA Laser Beam Interaction Workshop, NY, Stony Brook, June 11-15, 2001 (these proceedings).
- [23] N.F.Shulga, S.N.Dobrovolskii, *JETP Lett.* **90** (2000) 579.
- [24] X.Artru, et al., *Nucl. Instr. And Meth. A* **410** (1998) 148.